

ARTICLES

Control-parameter-dependent Swift-Hohenberg equation as a model for bioconvection patterns

J. Lega

Department of Mathematics, University of Arizona, Tucson, Arizona 85721

N. H. Mendelson

Department of Molecular and Cellular Biology, University of Arizona, Tucson, Arizona 85721

(Received 21 December 1998)

We consider a complex Swift-Hohenberg equation with control-parameter-dependent coefficients and use it as a model to describe dynamical features seen in an experimental bacterial bioconvection pattern. In particular, we give numerical results showing the development of a phase-unstable pattern behind a moving front. [S1063-651X(99)07906-4]

PACS number(s): 45.70.Qj, 87.18.Hf, 47.54.+r

I. INTRODUCTION

Patterns form in various physical systems, and at various scales. Whether they occur in fluids subject to temperature gradients [1–11] or to parametric forcings [12,13], in Couette-Taylor flows [14], in directional solidification [15], in chemical reactors [16–19], in liquid crystals [20–22], in granular layers [23–26], in passive and active optical devices [27–37], or in biological systems [38–54], they result from the nonlinear competition between linearly growing, spatially and/or temporally periodic modes. This competition can be described in terms of envelope equations, which capture the pattern dynamics near threshold (for a review, see, for instance, [55] or [56]). These equations are the partial-differential-equation analogs of normal forms for dynamical systems, and have been successfully used to analyze patterns and their defects. Sometimes, these equations are formally derived from the microscopic description of the system under consideration, in which case the properties of a particular pattern can be quantitatively related to physical parameters. More often, amplitude equations are written on the basis of symmetry arguments, and used to analyze generic pattern behaviors [57–59].

Formally speaking, amplitude equations are only valid near threshold. As far as modeling is concerned, it is, however, generally accepted that they give a good qualitative description of a pattern at a finite distance from threshold, as long as this pattern undergoes instabilities which are consistent with the amplitude equation approximation. For instance, phase instabilities are reasonably captured by amplitude equations since the latter allow the phase of the order parameter to vary. On the contrary, a new set of amplitude equations needs to be introduced in order to describe secondary instabilities involving harmonics of the basic structure [60]. In the case of a bifurcation towards a one-dimensional traveling wave pattern, an amplitude equation description in terms of two counterpropagating waves of wave vectors $\pm k_c$ can be expected to be valid at a finite distance μ from thresh-

old only if the neutral stability curve $\mu = \mu(k)$ [see Fig. 1(a)] shows a clearly marked minimum at $k = \pm k_c$. If not, as is generically the case if $\mu_c = \mu(0)$ is small [see Fig. 1(b)], the fact that $k_c^2 \approx \mu_c$ is comparable to the distance from threshold must be taken into account in the multiple scale analysis used to describe the bifurcation. As a consequence, a different order parameter equation, namely, the complex Swift-Hohenberg equation, should be used to model the near-threshold dynamics. In scaled variables, this equation reads

$$\frac{\partial \psi}{\partial t} = \mu \psi - (1 + i\alpha)(\Omega + \nabla^2)^2 \psi - (1 + i\beta)|\psi|^2 \psi + i\gamma \nabla^2 \psi, \tag{1}$$

where ψ is a complex order parameter and all of the other coefficients are real. Such an equation was considered as a model for a passive optical system driven by an external field in [61]. In [62,63], it was derived from the Maxwell-Bloch

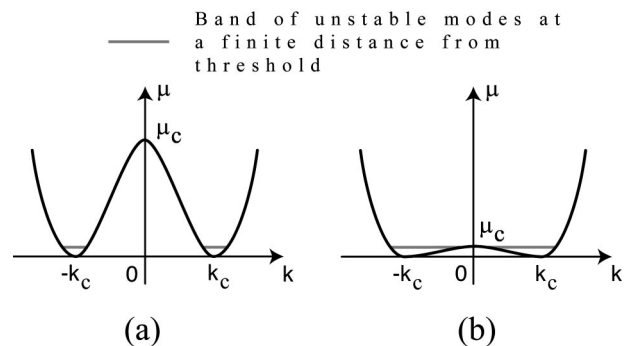


FIG. 1. Sketch of the neutral stability curve $\mu(k)$ giving the wave number k of marginal Fourier modes as a function of the distance from threshold μ . (a) When $\mu > 0$, modes of wave number k in a band centered about k_c experience growth. (b) When $\mu_c = \mu(0)$ is comparable to k_c^2 , the relative width $\Delta k/k_c$ of the band of unstable modes is of order one for small values of μ , thereby limiting the region of validity of amplitude equations.

equations describing the dynamics of two-level lasers and thereby shown to provide a universal description of class A and C lasers near threshold. Later, this approach was extended to optical parametric oscillators in [64,65].

Historically, the cubic Swift-Hohenberg equation with real coefficients and a real order parameter ψ was described in [66] as a pattern-forming model for Rayleigh-Bénard convection. Later, a quadratic version thereof was also considered to model competition between hexagons and squares (see, e.g., [67]). Recently, a Swift-Hohenberg equation coupled to a mean-flow equation was shown to describe patterns in rotating convection [68]. More generally, both the real and complex Swift-Hohenberg equations and their generalizations have been used as generic pattern-forming models for one-dimensional periodic patterns [69–73].

In this paper, we are interested in the dynamics of the complex Swift-Hohenberg equation (1) when the parameters involved in the equation depend on the distance μ from the bifurcation threshold. We consider that $\Omega = k_c^2$ is positive and varies linearly and quadratically in μ , whereas the other parameters depend on μ linearly. Such an approximation can be obtained by keeping the first terms of the Taylor expansion of the parameters in the distance from threshold (μ). We do not, however, include in the Swift-Hohenberg equation higher order nonlinear terms in ψ or its derivatives, except for one quintic term which might be needed in the case of a subcritical bifurcation. In other words, we do not consider the complex Swift-Hohenberg equation with control-parameter-dependent coefficients as the result of a multiple scales analysis, but we take it as a simple pattern-forming model for which the preferred wave number k_c and the stability properties of plane wave solutions above threshold depend on the distance from threshold. This is a very natural assumption, and this situation is likely to occur in many physical systems driven far from equilibrium by some external forcing.

As a motivation, we describe below an experimental bioconvection pattern [74], in which bacteria multiply as the pattern evolves, thereby changing the control parameter as the colony develops. We then consider the general complex Swift-Hohenberg equation

$$\frac{\partial \psi}{\partial t} = (\mu + i\nu)\psi - (\alpha_r + i\alpha_i)(k_c^2 + \nabla^2)^2 \psi - (\beta_r + i\beta_i)|\psi|^2 \psi + i\gamma \nabla^2 \psi - (\zeta_r + i\zeta_i)|\psi|^4 \psi, \quad (2)$$

and use it to model this bioconvection pattern. We add quintic terms in order to leave open the possibility of a subcritical bifurcation and use the unscaled version of Eq. (1) since it provides a convenient way to take into account the dependence of the various coefficients on the control parameter μ .

The paper is organized as follows. In Sec. II, we show how a pattern arises as a solution of Eq. (2) when μ is positive and find the region of stability of plane wave solutions in the k - μ plane by means of a phase diffusion equation. In Sec. III, we discuss the bioconvection experiment and how the above equation can be used as a model which incorporates bacterial growth and migration. Section IV is devoted to numerical simulations of the model and Sec. V discusses possible implications of these results for the analysis of bioconvection.

II. THE COMPLEX SWIFT-HOHENBERG EQUATION WITH CONTROL-PARAMETER-DEPENDENT COEFFICIENTS

We consider the complex Swift-Hohenberg equation (2). At this stage, we let ψ be a function of both horizontal variables x and y , but the numerics will be done for a one-dimensional pattern. Equation (2) has a simple solution, $\psi = 0$, which corresponds to the absence of structure. When μ is larger than 0, an instability occurs and a spatially periodic pattern is formed. Indeed, perturbations of $\psi = 0$ with wave number k grow or decay at a linear rate given by

$$\sigma(k) = \mu + i\nu - (\alpha_r + i\alpha_i)(k_c^2 - k^2)^2 - i\gamma k^2,$$

and the modes experiencing maximum growth have a wave number $k = \pm k_c$, and a frequency $\omega = \nu - \gamma k_c^2$. The cubic or quintic nonlinear terms of Eq. (2) saturate this instability. In particular, traveling wave solutions of Eq. (2) can be found, which read $\psi = R \exp[i(\omega t + \vec{k} \cdot \vec{r})]$, where

$$\begin{aligned} 0 &= \mu - \alpha_r(k^2 - k_c^2)^2 - \beta_r R^2 - \zeta_r R^4, \\ \omega &= \nu - \alpha_i(k^2 - k_c^2)^2 - \beta_i R^2 - \zeta_i R^4 - \gamma k^2, \end{aligned} \quad (3)$$

and $k = |\vec{k}|$. Depending on the values of the parameters of Eq. (2) and on the wave number k , these solutions may undergo a phase instability [75–81]. This instability can be analyzed, at least in the early stage of its development, by reducing Eq. (2) to a single equation for the phase of the complex quantity ψ . More precisely, when ψ is close to a traveling wave solution (3), we can write ψ as $\psi = R_0(k) \exp(i\theta) + \dots$ where $R_0(k)$ is a solution of Eq. (3), θ is such that $\vec{\nabla} \theta = \vec{k}$ varies slowly in space and time, and the dots stand for higher order corrections coming from the fact that $R_0(k) \exp(i\theta)$ is no longer an exact solution of the Swift-Hohenberg equation. Under these conditions, the phase θ satisfies a phase-diffusion equation, which reads at lowest order

$$\begin{aligned} \frac{\partial \theta}{\partial t} &= \omega(k) + \left[-2 \frac{\alpha_r b_r + \alpha_i b_i}{b_r} (k_c^2 - 3k^2) \right. \\ &\quad \left. + \frac{\gamma b_i}{b_r} - \frac{8k^2(k_c^2 - k^2)^2 \alpha_r^2 b_r^2 + b_i^2}{b_r R_0^2 b_r^2} \right] \frac{\partial^2 \theta}{\partial x^2} \\ &\quad + \left[-2 \frac{\alpha_r b_r + \alpha_i b_i}{b_r} (k_c^2 - k^2) + \frac{\gamma b_i}{b_r} \right] \frac{\partial^2 \theta}{\partial y^2}, \end{aligned} \quad (4)$$

where

$$b_r = \beta_r + 2\zeta_r R^2, \quad b_i = \beta_i + 2\zeta_i R^2,$$

R_0 is the amplitude of the traveling wave and is given in Eq. (3). In this equation, the x axis has been chosen parallel to the local wave vector \vec{k} and the y axis is therefore perpendicular to \vec{k} . Equation (4) is nonlinear in $\vec{\nabla} \theta$ since $\omega(k)$, given by Eq. (3) with $R = R_0(k)$, contains terms in $k^2 = |\vec{\nabla} \theta|^2$. The method used to obtain such an equation is a generalization to wave patterns [82] of the technique developed in [83]. In one space dimension, stable wave vectors are

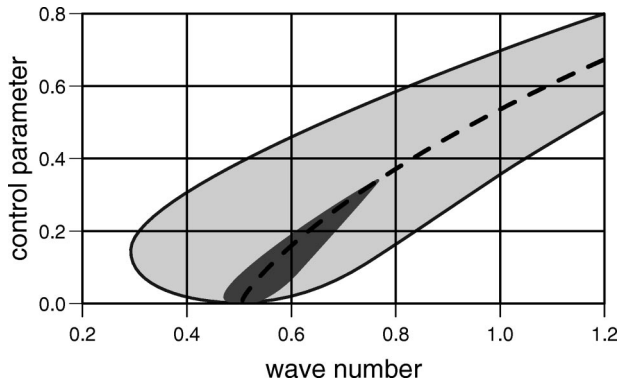


FIG. 2. Domain of existence of one-dimensional traveling waves (light gray) and Busse balloon (dark gray) for $\alpha_r=2.0+0.85\mu$, $\alpha_i=0.8+0.5\mu$, $\beta_r=1.0$, $\beta_i=-1.3-2.0\mu$, $k_c=0.5+0.5\mu+0.8\mu^2$, $\gamma=0.453$, and $\zeta_r=\zeta_i=0.0$. Units are arbitrary. The dashed curve gives the wave vector k which experiences maximum linear growth above threshold.

such that the coefficient $E(k, \mu)$ of $\partial^2 \theta / \partial x^2$ in the phase-diffusion equation is positive, and the width of the region of stability of plane wave solutions can therefore be adjusted by changing the parameters $\alpha_r, \alpha_i, \dots, \zeta_i$. In the absence of amplitude instabilities, this region is the analog of the Busse balloon [84] for convection patterns. Conversely, one can use Eq. (4) to choose the μ dependence of the coefficients of the Swift-Hohenberg equation (2) in order to produce Busse balloons of various shapes. For instance, Fig. 2 shows the stability domain of one-dimensional plane waves for $\alpha_r=2.0+0.85\mu$, $\alpha_i=0.8+0.5\mu$, $\beta_r=1.0$, $\beta_i=-1.3-2.0\mu$, $\gamma=0.453$, $\zeta_r=\zeta_i=0.0$, and $k_c=0.5+0.5\mu+0.8\mu^2$, numerically computed by finding those lines in the $k-\mu$ plane such that $E(k, \mu)=0$. It is seen that no traveling wave is stable if $\mu > \mu_B \approx 0.35$.

Equation (2) with control-parameter-dependent coefficients therefore appears as a simple, generic, pattern-forming system whose dynamic properties above threshold can be adjusted by an adequate choice of parameters. The following is an example of how such an equation can be used to model a bioconvection experiment.

III. EXPERIMENTAL RESULTS

Bioconvection occurs when unicellular organisms (bacteria, algae) gather at the surface of a fluid whose density is less than their own. As a consequence, the heavy layer of cells which forms atop the fluid may become unstable if the concentration of organisms gets too high. In a way similar to Rayleigh-Bénard convection, plumes of sinking and rising fluid are formed, but here the cells are advected by the fluid as they swim. This phenomenon was reported by Wager in 1911 [38], and Platt devised the name “bioconvection” [39]. The phenomenon has since been studied more extensively both analytically [40,85–90] and experimentally (see, e.g., [91,92,54]), and the interested reader may refer to the recent review articles by Pedley and Kessler [41,42], and to references therein. When viewed from above, bioconvection patterns in general appear to be square or hexagonal, and a tendency towards labyrinthine structures has also been seen (see, e.g., [38,91]). Although drifting of the pattern has

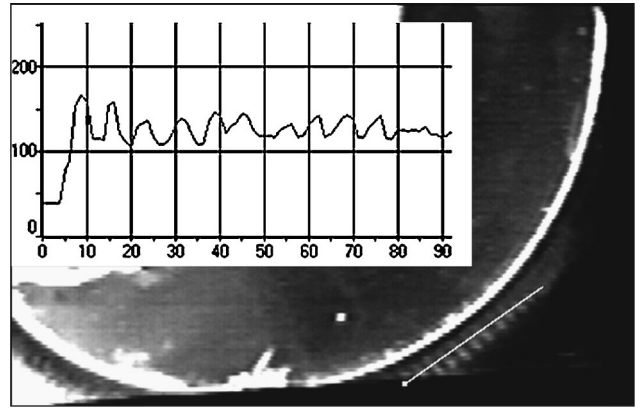


FIG. 3. Video frame showing the bioconvection pattern [74]. The inset gives the pattern intensity as a function of position along the line drawn on the video frame. (One unit on the x axis of the inset corresponds to 0.155 mm actual length. Units on the vertical axis are arbitrary.)

sometimes been observed [93], bioconvection structures are in general stationary. Various hydrodynamic models describing the coupling between the moving fluid and the swimming cells have been proposed [40,85–90], for different types of microscopic organisms. Bioconvection has indeed been observed in gravitactic, chemotactic, or phototactic organisms (see [41]). In each case, depending on the cell size and on the nature of their motion, a different model is required. To our knowledge, the only weakly nonlinear analysis of a bioconvection pattern is given in [90] for bacteria. It is shown that the bifurcation towards hexagons is stationary and supercritical.

In this paper, we are interested in a one dimensional, traveling wave bioconvection structure, which is produced by a culture of *Bacillus subtilis*. To our knowledge, this pattern is the first traveling wave bioconvection pattern which has been analyzed. The details are given in [74], where the bacterial strains and the experimental setup are described. The pattern is forced to be one-dimensional by restricting bioconvection to the meniscus formed by a nutritive fluid near a solid wall, made of either agar or plastic. It is shown in [74] that traveling waves are easily produced each time motile strains OI2836 or OI1085 of *Bacillus subtilis* swim in the meniscus that forms near a flat or curved wall. What makes this bioconvection pattern particularly interesting is that, as described below, it exhibits many dynamical features. In particular, its properties evolve in time since the bacteria multiply as they swim. Moreover, it develops behind a front created by a cloud of cells swimming towards fresh nutrients, and the wave number of the structure behind the front is such that an instability develops. Space-time dislocations and eventually spatiotemporal disorder are then observed.

Figure 3 shows a circular agar disk, together with the one-dimensional bioconvection pattern in the bottom-right corner. Although bacteria are present away from the agar disk, the pattern only forms in the meniscus near the disk, where the fluid is deeper. The inset gives a cross section of the pattern (white line at the bottom-right corner), which has a wavelength of about 1 mm. Figure 4 shows a space-time diagram of the evolution of the structure, where many dynamical features can be seen. First, a front between regions

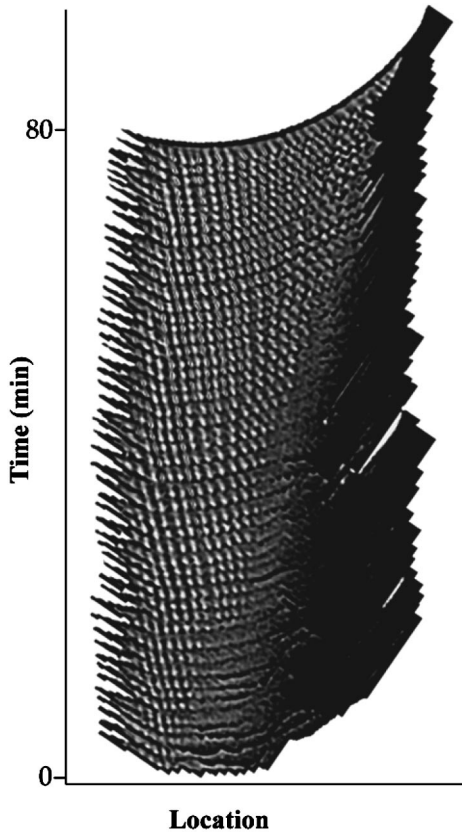


FIG. 4. Spatiotemporal diagram showing the evolution of the pattern [74]. The same portion of 51 video frames (one of them is shown in Fig. 3) was selected and transferred by computer to form a composite figure spanning 80 minutes in real time.

with bacteria (on the left) and without bacteria (on the right) propagates from left to right in the figure at a speed ≈ 0.225 mm/min, which is constant on average. The fresh fluid appears black in the figure, whereas the culture of bacteria is in dark gray. Behind this front, a pattern is formed (alternating dark and light gray stripes), which travels away from the front. This pattern is unstable since new stripes appear between existing ones, and eventually degenerates towards spatiotemporal disorder [74] (not shown in the figure).

Global regulation in the form of such a dynamic pattern is quite remarkable for a culture of microorganisms. It results from the interplay of cells swimming up and towards fresh nutrients, fluid motion due to bioconvection, and expansion of the cell population. We understand this phenomenon as follows: behind the propagating front, the average density of bacteria reaches the critical threshold for bioconvection. The pattern which is formed is regulated by the growth of the culture and the average distribution of cells, in the sense that the local wave number depends on the cell density and on the cloud shape. As the culture grows, the wavelength of the pattern is adjusted by insertion of new stripes between existing ones and when the cell density gets too high, a threshold is reached above which no stable structure can be sustained. The pattern then decays into a space-time disordered state.

To illustrate these ideas, we now develop a pattern-forming model in the form of the complex Swift-Hohenberg equation discussed above, driven by a space- and time-dependent control parameter, which represents the average

density of cells. Because the coefficients of the Swift-Hohenberg equation are control-parameter dependent, the properties of the pattern and its stability change as the control parameter gets larger. Since bioconvection starts when the layer of cells at the surface of the fluid becomes too heavy, the control parameter μ must be proportional to the difference between the average cell concentration ρ and some critical value ρ_c , above which bioconvection appears. Because the culture forms a cloud propagating from left to right in Fig. 4, ρ should be a function of space, which vanishes ahead of the front. The exact form of this front depends on the properties of the fluid and of the bacteria, but, as a first approximation, we can use the analytic shape found by Keller and Segel in [94], which reads

$$\rho = \rho_0 \frac{\exp[-(x-ct)/D]}{\{1 + \exp[-(x-ct)/D]\}^{r/(r-1)}}.$$

This approximation is justified since the bacteria are chemotactic towards fresh nutrients. The parameters are the ratio D between the motility parameter and the front speed c , and the parameter r describing the scaled slope of the chemotactic coefficient as a function of the inverse of the nutrient concentration. Moreover, since the culture is growing as it propagates, we add a multiplicative term which describes exponential growth behind the front, and thus define ρ as

$$\rho(x,t) = \rho_0 \frac{\exp[-(x-ct)/D]}{\{1 + \exp[-(x-ct)/D]\}^{r/(r-1)}} \times \exp\left[\lambda t \tanh\left(-\frac{x-ct}{D} - \ln(r-1)\right)\right]. \quad (5)$$

No saturation of the exponential growth is included in this formula since we describe the phenomenon in the initial stage of the culture development (a typical doubling time is 90 minutes). The control parameter μ is given by the difference $\rho - \rho_c$, where ρ_c is a constant value for the threshold of bioconvection. When $\rho(x,t)$ exceeds ρ_c , which happens at a fixed distance behind the front, a pattern grows.

Next, we need to choose the parameters $\alpha_r, \alpha_i, \dots, \zeta_i$ of Eq. (2). We assume that these parameters, as well as the preferred wave vector k_c , depend on the distance from threshold μ . The function $k_c(\mu)$ is chosen as $k_c = 0.5 + 0.5\mu + 0.8\mu^2$, so that the wavelength of the mode experiencing maximum growth decreases as μ gets larger. In other words, stripes tend to get closer to one another as the culture grows. The coefficients $\alpha_r, \alpha_i, \dots, \zeta_i$ are chosen in order to have a small Busse balloon. More precisely, we want the band of stable wave vectors k , which is centered around k_c , to get narrower and eventually shrink to zero as μ is increased above some threshold μ_B , as shown in Fig. 2. This will make the pattern unstable as the culture develops, and eventually lead to spatiotemporal disorder. Indeed, since $\rho(x,t)$ grows in time, there will be a time when the difference $\rho(x,t) - \rho_c$ gets above μ_B at some point x . When the size of the region (in x) where this happens gets large enough to sustain spatiotemporal disorder, the pattern will break and get disorganized at a small scale.

Many other parameter choices can be made. It should, however, be emphasized that the generic behavior of the pattern does not depend on the particular parameter values used in the model, but on the following crucial points. First, the pattern is driven by a time- and space-dependent control parameter ($\mu = \rho - \rho_c$). Second, its properties change as the control parameter is increased (due to the dependence of $\alpha_r, \alpha_i, \dots, \zeta_i$ on μ). Third, the structure degenerates towards spatiotemporal disorder (i.e., the Busse balloon gets narrower as μ is increased).

IV. NUMERICAL SIMULATIONS

We now show numerical simulations of the model with the parameters given above, together with $\rho_c = 0.3$, and $\rho_0 = 0.9$, $D = 10.0$, $r = 10.0$, $\lambda = 0.001$ for the shape of the driving front. The front speed $c = 0.3$ (arbitrary units) and the frequency $\nu = -0.1$ are chosen so that the relative scales in the space-time diagram are similar to what is seen in the experiment. The simulation is performed in one space dimension, in a box of size $L_x = 350$ (arbitrary units), and with a time step $dt = 0.001$. We use a spectral-like compact finite difference scheme [95] and nonreflecting boundary conditions [96]. The data are evolved by means of a fourth order Runge-Kutta scheme. The simulation has an interactive interface built with the visual graphical software AVS (Advanced Visual Systems), which makes it easier to choose the parameters which give the desired shape for the Busse balloon.

Figure 5 is a gray scale spatiotemporal diagram of a quantity representing the total concentration of bacteria, namely, $\rho(x, t) + \text{Re}[\psi(x, t)]$. Indeed, $\text{Re}[\psi(x, t)]$ or a scaled version thereof is the correction to the average density $\rho(x, t)$ due to the presence of the pattern. The region without bacteria is on the right. One can clearly see the driving front moving at a constant speed $c = 0.3$, and the pattern forming behind this front. Space-time dislocations are observed behind the front and, as we had expected, the pattern eventually becomes disordered.

The parameters are such that the bifurcation is a forward bifurcation, since $\beta_r > 0$ and $\zeta_r = \zeta_i = 0$. At threshold, $\omega(k_c) = \nu - \gamma k_c^2 = -0.1 - 0.543(0.5)^2 = -0.21$, and

$$\frac{1}{k} \frac{d\omega}{dk} \Big|_{k_c} = -2\gamma < 0,$$

so that amplitude perturbations travel in a direction opposite to the direction of travel of the pattern. In particular, if the stripes travel away from the front, amplitude perturbations will travel towards the front. However, the situation is reversed when μ is increased, as can be seen from the propagation of space-time disorder away from the front in Fig. 5.

Figure 6 shows the quantities $\rho(x, t)$ (top curve) and $|\psi(x, t)|$ (bottom curve) as functions of space, at time $t = 262.5$ (arbitrary units). It is seen that the pattern, which corresponds to a nonzero ψ , forms at a given distance behind the front, and that its amplitude is related to the front shape. Insertion of new stripes between existing ones, which look like dislocations in the spatiotemporal diagram of Fig. 5, occurs when $|\psi(x, t)|$ vanishes. The dip in the profile of $|\psi|$

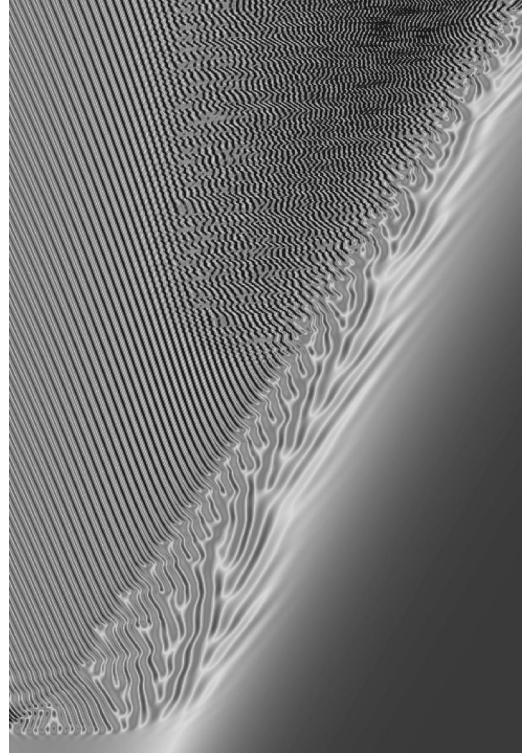


FIG. 5. Spatiotemporal diagram showing the evolution of $\rho(x, t) + \text{Re}[\psi(x, t)]$ as a function of time between $t = 0$ and $t \approx 965$ (arbitrary units) [74]. The parameters used to produce this diagram are (arbitrary units) $\rho_c = 0.3$, $\alpha_r = 2.0 + 0.85\mu$, $\alpha_i = 0.8 + 0.5\mu$, $\beta_r = 1.0$, $\beta_i = -1.3 - 2.0\mu$, $k_c = 0.5 + 0.5\mu + 0.8\mu^2$, $\gamma = 0.453$, $\zeta_r = \zeta_i = 0.0$, $\nu = -0.1$, $\rho_0 = 0.9$, $c = 0.3$, $D = 10.0$, $r = 10.0$, $\lambda = 0.001$, $L_x = 350.0$, and $dt = 0.001$. Time increases upward.

around $x = 90$ shows that such an event had just occurred, or was about to occur when the snapshot of Fig. 6 was taken.

Figure 7 shows $\rho(x, t)$ and $\text{Re}[\psi(x, t)]$ at a later time, $t = 965.5$. The real part of ψ describes the periodic structure seen in the stripe pattern. From this figure, one can see that $\rho(x, t)$ given by Eq. (5) decays regularly on the left of the

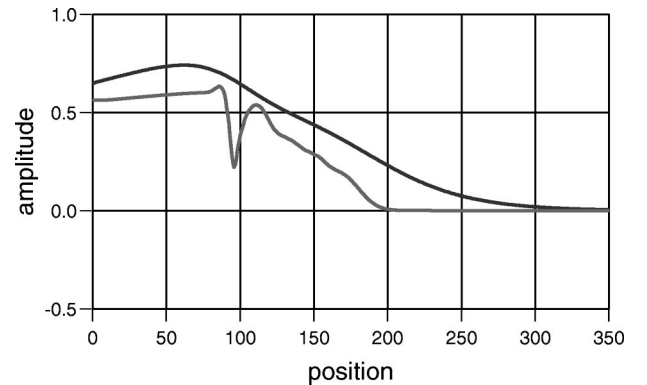


FIG. 6. Field profiles at $t = 262.5$ (arbitrary units). The top curve is a plot of the driving front as a function of x , and the bottom curve shows $|\psi(x)|$. The parameters used to produce this plot are (arbitrary units) $\rho_c = 0.3$, $\alpha_r = 2.0 + 0.85\mu$, $\alpha_i = 0.8 + 0.5\mu$, $\beta_r = 1.0$, $\beta_i = -1.3 - 2.0\mu$, $k_c = 0.5 + 0.5\mu + 0.8\mu^2$, $\gamma = 0.453$, $\zeta_r = \zeta_i = 0.0$, $\nu = -0.1$, $\rho_0 = 0.9$, $c = 0.3$, $D = 10.0$, $r = 10.0$, $\lambda = 0.001$, $L_x = 350.0$, and $dt = 0.001$.

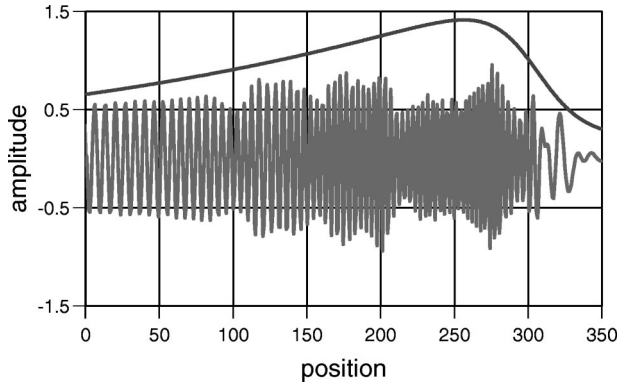


FIG. 7. Fields at $t=965.5$ (arbitrary units). The top curve is a plot of the driving front as a function of x , and the bottom curve shows $\text{Re}\psi(x)$. The parameters used to produce this plot are (arbitrary units) $\rho_c=0.3$, $\alpha_r=2.0+0.85\mu$, $\alpha_i=0.8+0.5\mu$, $\beta_r=1.0$, $\beta_i=-1.3-2.0\mu$, $k_c=0.5+0.5\mu+0.8\mu^2$, $\gamma=0.453$, $\zeta_r=\zeta_i=0.0$, $\nu=-0.1$, $\rho_0=0.9$, $c=0.3$, $D=10.0$, $r=10.0$, $\lambda=0.001$, $L_x=350.0$, and $dt=0.001$.

front, which explains the regularity of the periodic structure on the left of Fig. 7 and of the spatiotemporal diagram of Fig. 5. It can also be seen in this figure that the wave number k of the pattern is driven by the shape of the front.

Finally, we show another space-time diagram in Fig. 8, for which the parameters are the same as before, except that $\rho_c=0.2$, which makes the pattern grow faster, and $D=9.43$,

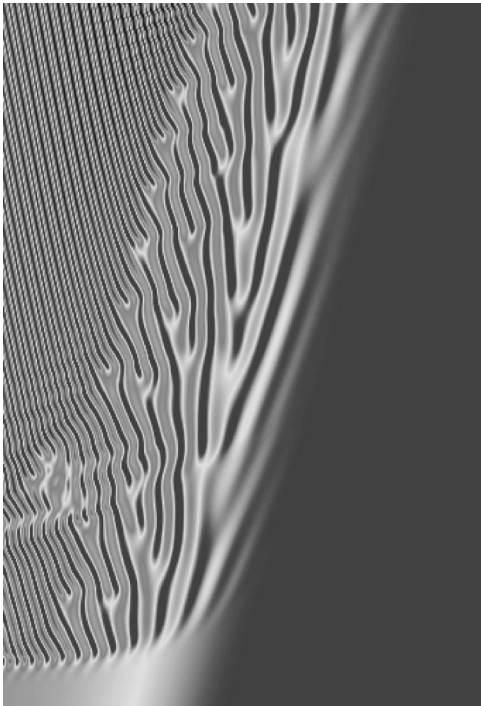


FIG. 8. Spatiotemporal diagram showing the evolution of $\rho(x,t)+\text{Re}[\psi(x,t)]$ as a function of time, between $t=0$ and $t=373.5$ (arbitrary units). Only part of the field in the x direction ($42 < x < 280$) is shown. The parameters used to produce this diagram are (arbitrary units) $\rho_c=0.2$, $\alpha_r=2.0+0.85\mu$, $\alpha_i=0.8+0.5\mu$, $\beta_r=1.0$, $\beta_i=-1.3-2.0\mu$, $k_c=0.5+0.5\mu+0.8\mu^2$, $\gamma=0.453$, $\zeta_r=\zeta_i=0.0$, $\nu=-0.1$, $\rho_0=0.9$, $c=0.3$, $D=9.43$, $r=10.0$, $\lambda=0.001$, $L_x=350.0$, and $dt=0.001$. Time increases upward.

which slightly changes the shape of the front. Only the region near the front is shown. The way new stripes get inserted between existing ones reproduces the global regulation of the experimental pattern remarkably well.

The essential message of these numerical experiments is that the simple pattern-forming model given by Eqs. (2) and (5) is sufficient to reproduce and understand the complexity of the experimental bacterial pattern. Two hypotheses were made to construct this model. First we assumed that bioconvection takes the form of an oscillatory instability which occurs when the average cell concentration gets above a fixed threshold, whence the use of a complex Swift-Hohenberg equation. Second, we considered that the culture in the propagating cloud was growing in time, which in turn led to an instability of the pattern, whence the use of control-parameter-dependent coefficients in Eq. (2).

V. DISCUSSION

The complex Swift-Hohenberg equation (2) considered in this paper gives a generic description of traveling wave patterns which develop above a Hopf bifurcation (as opposed to a drift bifurcation [97]). The introduction of control-parameter-dependent coefficients turns this equation into a very general model which can adequately describe Busse balloons of various shapes. The stability results as well as the dynamical behaviors discussed here are therefore likely to apply to many other traveling wave patterns exhibiting spatiotemporal behaviors, such as those recently observed in some convection experiments [98]. Equation (2) is also a good model to study wave number selection in a pattern driven by a space-dependent control parameter, as is the case here (in particular, see Fig. 7). Such an analysis is, however, beyond the scope of this paper.

It is also interesting to draw some conclusions about what one can learn, from a biological point of view, from the above model. First, the strains of *Bacillus subtilis* used in the experiment are believed not to exchange signals with one another that influence swimming. The global behavior which corresponds to the existence of a pattern, as well as the complexity of the structure, could have suggested that signalling between cells was necessary. Moreover, the presence of dislocations in the spatiotemporal diagram could have been interpreted as a form of global regulation, where the cells would know the history of the pattern. What the Swift-Hohenberg model suggests is that space-time dislocations and later space-time disorder are simply the signature of a phase instability of the structure behind the moving front, and that the same phenomenon would be observed in any pattern which would undergo a similar type of instability.

Second, the experimental pattern clearly exhibits traveling waves, which means that the bifurcation towards bioconvection is oscillatory. From a hydrodynamics point of view, this implies that the vertical distribution of cells swimming in a fluid at rest before bioconvection occurs undergoes a Hopf bifurcation. This possibility was recently discussed for phototactic algae by Vincent and Hill in [88]. However, because our pattern is made one dimensional by being restricted to the meniscus of the fluid near a vertical boundary, surface-tension effects could be relevant and could in fact trigger traveling waves, as they do for thermal convection [99]. It

would therefore be very instructive to study this pattern in narrow channels, where such effects could be better controlled.

Before any hydrodynamic model can be made, the role of surface tension in the bioconvection process must be assessed (in two dimensions, it is considered as negligible [100]). Moreover, the way cell motion couples to fluid flows must be investigated. To this end, one could use markers and look at vertical slices of the fluid, as is commonly done in fluid flow experiments (see, e.g., [101]). Such experimental results could then be compared to theoretical models for the swimming of flagellated organisms, as, for instance, described in [102], and help to construct a hydrodynamic model for the experimental pattern studied here.

If such a model were available, a Swift-Hohenberg equa-

tion like Eq. (2) could then be derived, along lines similar to those followed in [62,63] for laser systems and [68] for rotating convection. This would give us quantitative information on the nature of the bifurcation (e.g., Hopf) which leads to the traveling wave pattern described in this paper, and on the way it saturates (i.e., subcritically or supercritically).

ACKNOWLEDGMENTS

This work was partially supported by a research grant from the National Center for Research Resources (NIH) to N.H.M. We are indebted to S. D. Whitworth for excellent technical assistance, and to J. O. Kessler for discussions concerning bioconvection in *B. subtilis*.

-
- [1] H. Bénard, Ann. Chim. Phys. **23**, 62 (1901).
- [2] P. Bergé and M. Dubois, J. Phys. (France) Lett. **40**, 505 (1979).
- [3] D. Bensimon, P. Kolodner, C. M. Surko, H. Williams, and V. Croquette, J. Fluid Mech. **217**, 441 (1990).
- [4] C. M. Surko and P. Kolodner, in *Nonlinear Structures in Physical Systems. Pattern Formation, Chaos and Waves*, Proceedings of the Second Woodward Conference, edited by Lui Lam and H.C. Morris (Springer-Verlag, Berlin, 1990), pp. 147–165.
- [5] E. Moses and V. Steinberg, Phys. Rev. A **43**, 707 (1991).
- [6] F. Zhong, R. Ecke, and V. Steinberg, Physica D **51**, 596 (1991).
- [7] E. Kaplan and V. Steinberg, Phys. Rev. A **46**, R2996 (1992).
- [8] E. Bodenschatz, D. S. Cannell, J. R. de Bruyn, R. Ecke, Y. C. Hu, K. Lerman, and G. Ahlers, Physica D **61**, 77 (1992).
- [9] E. Pampaloni, C. Perez-Garcia, L. Albavetti, and S. Ciliberto, J. Fluid Mech. **234**, 393 (1992).
- [10] G. Ahlers, in *25 Years of Non-Equilibrium Statistical Mechanics*, Proceedings of the 13th Sitges Conference, edited by J. J. Brey, J. Marro, J. M. Rubi, and M. San Miguel (Springer-Verlag, Berlin, 1995), pp. 91–124.
- [11] M. Assenheimer and V. Steinberg, Phys. Rev. Lett. **76**, 756 (1996).
- [12] S. Douady, S. Fauve, and O. Thual, Europhys. Lett. **10**, 309 (1989).
- [13] W. S. Edwards and S. Fauve, J. Fluid Mech. **278**, 123 (1994).
- [14] C. D. Andereck, S. S. Liu, and H. L. Swinney, J. Fluid Mech. **164**, 155 (1986).
- [15] M. Ginibre, S. Akamatsu, and G. Faivre, Phys. Rev. E **56**, 780 (1997).
- [16] A. T. Winfree, in *Oscillations and Traveling Waves in Chemical Systems*, edited by R. J. Field and M. Burger (Wiley, New York, 1985), pp. 441–472.
- [17] V. Castets, E. Dulos, J. Boissonade, and P. De Kepper, Phys. Rev. Lett. **64**, 2953 (1990).
- [18] Q. Ouyang and H. L. Swinney, Chaos **1**, 411 (1991).
- [19] Q. Ouyang and H. L. Swinney, Nature (London) **352**, 610 (1991).
- [20] A. Joets and R. Ribotta, J. Phys. (France) **47**, 595 (1986).
- [21] A. Joets and R. Ribotta, Phys. Rev. Lett. **60**, 2164 (1988).
- [22] H. Richter, A. Buka, and I. Rehberg, Phys. Rev. E **51**, 5886 (1995).
- [23] C. Laroche, S. Douady, and S. Fauve, J. Phys. (France) **50**, 699 (1989).
- [24] S. Douady, S. Fauve, and C. Laroche, Europhys. Lett. **8**, 621 (1989).
- [25] F. Melo, P. Umbanhowar, and H. L. Swinney, Phys. Rev. Lett. **72**, 172 (1994).
- [26] F. Melo, P. Umbanhowar, and H. L. Swinney, Phys. Rev. Lett. **75**, 3838 (1995).
- [27] J. Opt. Soc. Am. B. **5**, (5) (1988), special issue on Nonlinear Dynamics of Lasers, edited by D. K. Bandy, A. N. Oraevsky, and J. R. Tredicce.
- [28] Chaos Solitons Fractals **4**, (819) (1994), special issue on Nonlinear Optical Structures, Patterns, Chaos, edited by L. A. Lugiato and M. S. El Naschie.
- [29] R. Macdonald and H. J. Eichler, Opt. Commun. **89**, 289 (1992).
- [30] S. A. Akhmanov, M. A. Vorontsov, V. Yu. Ivanov, A. V. Larichex, and N. I. Zheleznykh, J. Opt. Soc. Am. B **9**, 78 (1992).
- [31] B. Thüring, R. Neubecker, and T. Tschudi, Opt. Commun. **102**, 111 (1993).
- [32] G. Grynberg, A. Maître, and A. Petrossian, Phys. Rev. Lett. **72**, 2379 (1994).
- [33] T. Ackemann and W. Lange, Phys. Rev. A **50**, R4468 (1994).
- [34] M. Brambilla, F. Battipede, L. A. Lugiato, V. Penna, F. Prati, C. Tamm, and C. O. Weiss, Phys. Rev. A **43**, 5090 (1991).
- [35] D. Dangoisse, D. Hennequin, C. Lepers, E. Louvergneaux, and P. Glorieux, Phys. Rev. A **46**, 5955 (1992).
- [36] F. T. Arecchi, S. Boccaletti, G. Giacomelli, G. P. Puccioni, P. L. Ramazza, and S. Residori, Physica D **61**, 25 (1992).
- [37] D. Hennequin, L. Dambly, D. Dangoisse, and P. Glorieux, J. Phys. III **4**, 2459 (1994).
- [38] H. Wager, Philos. Trans. R. Soc. London, Ser. B **201**, 333 (1911).
- [39] J. R. Platt, Science **133**, 1766 (1961).
- [40] S. Childress, M. Levandowsky, and E. A. Spiegel, J. Fluid Mech. **69**, 595 (1975).
- [41] T. J. Pedley and J. O. Kessler, Annu. Rev. Fluid Mech. **24**, 313 (1992).

- [42] T. J. Pedley and J. O. Kessler, *Sci. Prog.* **76**, 105 (1992).
- [43] J. D. Murray, *Mathematical Biology* (Springer-Verlag, Berlin, 1989).
- [44] E. O. Budrene and H. C. Berg, *Nature (London)* **349**, 630 (1991).
- [45] E. O. Budrene and H. C. Berg, *Nature (London)* **376**, 49 (1995).
- [46] Y. Blat and M. Eisenbach, *J. Bacteriol.* **177**, 1683 (1995).
- [47] E. Ben-Jacob, I. Cohen, O. Shochet, I. Aranson, H. Levine, and L. Tsimring, *Nature (London)* **373**, 566 (1995).
- [48] L. Tsimring and H. Levine, *Phys. Rev. Lett.* **75**, 1859 (1995).
- [49] T. Höfer, J. A. Sherratt, and P. K. Maini, *Physica D* **85**, 425 (1995).
- [50] J. A. Shapiro, *BioEssays* **17**, 597 (1995).
- [51] S. Kondo and R. Asal, *Nature (London)* **376**, 765 (1995).
- [52] T. Höfer and P. K. Maini, *Nature (London)* **380**, 678 (1996).
- [53] N. H. Mendelson and B. Salhi, *J. Bacteriol.* **178**, 1980 (1996).
- [54] I. M. Janosi, J. O. Kessler, and V. K. Horvath, *Phys. Rev. E* **58**, 4793 (1998).
- [55] M. C. Cross and P. C. Hohenberg, *Rev. Mod. Phys.* **65**, 851 (1993).
- [56] A. C. Newell, T. Passot, and J. Lega, *Annu. Rev. Fluid Mech.* **25**, 399 (1993).
- [57] *New Trends in Nonlinear Dynamics and Pattern-forming Phenomena—The Geometry of Nonequilibrium*, edited by P. Coulet and P. Huerre (Plenum Press, New York, 1990).
- [58] *Nonlinear Evolution of Spatio-Temporal Structures in Dissipative Continuous Systems*, edited by F. H. Busse and L. Kramer (Plenum Press, New York, 1990).
- [59] *Pattern Formation and Instabilities in Continuous Dissipative Systems*, edited by H. R. Brand, H. Flaschka, and A. C. Newell, special issue of *Physica D* **97**, Nos. 1–3 (1996).
- [60] P. Coulet and G. Iooss, *Phys. Rev. Lett.* **64**, 866 (1990).
- [61] M. Tlidi, M. Giorgiou, and P. Mandel, *Phys. Rev. A* **48**, 4605 (1993).
- [62] J. Lega, J. V. Moloney, and A. C. Newell, *Phys. Rev. Lett.* **73**, 2978 (1994).
- [63] J. Lega, J. V. Moloney, and A. C. Newell, *Physica D* **83**, 478 (1995).
- [64] S. Longhi and A. Geraci, *Phys. Rev. A* **54**, 4581 (1996).
- [65] V. J. Sanchez-Morcillo, E. Roldan, G. J. de Valcarcel, and K. Staliunas, *Phys. Rev. A* **56**, 3237 (1997).
- [66] J. Swift and P. C. Hohenberg, *Phys. Rev. A* **15**, 319 (1977).
- [67] M'F. Hilali, S. Métens, P. Borckmans, and G. Dewel, *Phys. Rev. E* **51**, 2046 (1995).
- [68] Y. Ponty, T. Passot, and P. L. Sulem, *Phys. Rev. E* **56**, 4162 (1997).
- [69] M. Bestehorn and H. Haken, *Phys. Rev. A* **42**, 7195 (1990).
- [70] I. Aranson and L. Tsimring, *Phys. Rev. Lett.* **75**, 3273 (1995).
- [71] V. J. Sanchez-Morcillo and G. J. de Valcarcel, *Quantum Semiclass. Opt.* **8**, 919 (1996).
- [72] V. J. Sanchez-Morcillo, G. J. de Valcarcel, E. Roldan, and K. Staliunas, *Phys. Rev. E* **57**, 4911 (1998).
- [73] H. Sakaguchi and B. Malomed, *Physica D* **118**, 250 (1998).
- [74] N. H. Mendelson and J. Lega, *J. Bacteriol.* **180**, 3285 (1998).
- [75] W. Eckhaus, *Studies in Nonlinear Stability* (Springer-Verlag, New York, 1965).
- [76] A. C. Newell, in *Lectures in Applied Mathematics, Nonlinear wave Motion*, edited by A. C. Newell (American Mathematical Society, Providence, 1974), Vol. 15, pp. 157–163.
- [77] Y. Kuramoto and T. Tsuzuki, *Prog. Theor. Phys.* **55**, 356 (1976).
- [78] Y. Kuramoto, *Prog. Theor. Phys. Suppl.* **64**, 346 (1978).
- [79] Y. Pomeau and P. Manneville, *J. Phys. (France) Lett.* **23**, 609 (1979).
- [80] L. Kramer and W. Zimmerman, *Physica D* **16**, 221 (1985).
- [81] B. Jانياud, A. Pumir, D. Bensimon, V. Croquette, H. Richter, and L. Kramer, *Physica D* **55**, 269 (1992).
- [82] J. Lega, P. K. Jakobsen, J. V. Moloney, and A. C. Newell, *Phys. Rev. A* **49**, 4201 (1994).
- [83] M. C. Cross and A. C. Newell, *Physica D* **10**, 29 (1984).
- [84] F. H. Busse, *Rep. Prog. Phys.* **41**, 1929 (1978).
- [85] T. J. Pedley, N. A. Hill, and J. O. Kessler, *J. Fluid Mech.* **195**, 223 (1988).
- [86] N. A. Hill, T. J. Pedley, and J. O. Kessler, *J. Fluid Mech.* **208**, 509 (1989).
- [87] A. J. Hillesdon and T. J. Pedley, *J. Fluid Mech.* **324**, 223 (1996).
- [88] R. V. Vincent and N. A. Hill, *J. Fluid Mech.* **327**, 343 (1996).
- [89] M. A. Bees and N. A. Hill, *Phys. Fluids* **10**, 1864 (1998).
- [90] A. M. Metcalfe and T. J. Pedley, *J. Fluid Mech.* **370**, 249 (1998).
- [91] J. O. Kessler and M. F. Wojciechowski, in *Bacteria as Multicellular Organisms*, edited by J. A. Shapiro and M. Dworkin (Oxford University Press, New York, 1997), pp. 417–450.
- [92] J. O. Kessler and N. A. Hill, in *Physics of Biological Systems*, edited by H. Fryvbjerg, J. Hertz, M.H. Jensen, O.G. Mouritsen, and K. Sneppen, *Lecture Notes in Physics* Vol. 480 (Springer, Berlin, 1997).
- [93] J. O. Kessler (private communication).
- [94] E. F. Keller and L. A. Segel, *J. Theor. Biol.* **30**, 235 (1971).
- [95] S. K. Lele, *J. Comput. Phys.* **103**, 16 (1992).
- [96] R. L. Higdon, *SIAM (Soc. Ind. Appl. Math.) J. Numer. Anal.* **31**, 64 (1994).
- [97] S. Fauve, S. Douady, and O. Thual, *J. Phys. II* **1**, 311 (1991).
- [98] N. Mukolobwicz, A. Chiffaudel, and F. Daviaud, *Phys. Rev. Lett.* **80**, 4661 (1998).
- [99] S. H. Davis, *Annu. Rev. Fluid Mech.* **19**, 403 (1987).
- [100] J. O. Kessler (private communication).
- [101] O. Dauchot and F. Daviaud, *Phys. Fluids* **7**, 335 (1995).
- [102] M. S. Jones, L. Le Baron, and T. J. Pedley, *J. Fluid Mech.* **281**, 137 (1994).